

Interplay between electronic and atomic structures in the Si(557)-Au reconstruction from first principles

Sampsa Riiikonen^{1,2,*} and Daniel Sánchez-Portal^{2,3,†}

¹*Departamento de Física de Materiales, Facultad de Química, Universidad del País Vasco (UPV/EHU), Apartado 1072, 20080 San Sebastián, Spain*

²*Donostia International Physics Center (DIPC), Paseo Manuel de Lardizabal 4, 20018 San Sebastián, Spain*

³*Centro de Física de Materiales, Centro Mixto CSIC-UPV/EHU, Apartado 1072, 20080 San Sebastián, Spain*

(Received 7 March 2007; published 10 July 2007)

The quasi-one-dimensional Si(557)-Au reconstruction has attracted a lot of attention in recent years. We study here the interplay between the electronic and structural degrees of freedom in this system. Our calculations are in good agreement with recent experimental data obtained using scanning tunneling microscopy and spectroscopy both at room and low temperatures. Together with the quite successful description of the experimental band structure, these results give further support to the current structural model of the Si(557)-Au surface. We consider in detail the energetics and variation of the band structure as a function of the buckling of the step edge and its implications to explain the observed metal-insulator transition. Finally, we present the results of a first-principles molecular dynamics simulation of several picoseconds performed at room temperature. As expected, we find a strong oscillation of the step-edge atoms. The dynamics associated with other vibrational modes is also observed. Particularly apparent are the oscillations of the height of the restatoms and adatoms and the associated fluctuation of the Si–Au–Si bond angles along the gold chain. This mode, together with step-edge buckling, has a strong influence on the insulating and/or metallic character of the surface.

DOI: 10.1103/PhysRevB.76.035410

PACS number(s): 73.20.-r, 71.10.Pm, 71.30.+h, 81.07.Vb

I. INTRODUCTION

An interesting family of quasi-one-dimensional reconstructions is formed by the deposition of submonolayer amounts of gold on flat and vicinal Si(111) surfaces.^{1,2} These structures are characterized by the formation of ordered arrays of gold wires with cross sections of atomic dimensions. One of these systems, the Si(557)-Au reconstruction, has been intensively studied in recent years due to its intriguing electronic properties. The terraces of the Si(557)-Au surface have a width of ~ 19 Å, each of them containing a monatomic chain of gold atoms running parallel to the step edge. For this reason, the Si(557)-Au surface was proposed as a possible realization of a one-dimensional metal and has attracted much attention.^{1–18}

Angle resolved photoemission spectroscopy (ARPES) experiments observed two strongly dispersing one-dimensional electronic bands near the Fermi energy (E_F) in this surface. Segovia *et al.*⁴ first interpreted the appearance of these two proximal bands as a signature of the spin-charge separation in a Tomanaga-Luttinger liquid.^{19–21} Although this proposal was ruled out by later measurements,⁵ the origin of these two one-dimensional bands remained a mystery. It was proposed that they could be associated with two different types of wires in the substrate.^{5,8} The structure of the Si(557)-Au surface is relatively well established from x-ray diffraction measurements⁶ and density functional theory (DFT) calculations.^{7,10} This structure is shown in Fig. 1. Besides the monatomic gold chains, this reconstruction exhibits other one-dimensional structures suitable to give characteristic signals in photoemission. Each terrace contains a row of silicon adatoms and the step edge is reconstructed according to the so-called honeycomb chain structure.^{10,22} However, the two bands that dominate the spectrum of the Si(557)-Au have very similar dispersions and cross E_F at nearby points in

reciprocal space. Thus, it seems quite unlikely that they originate in wires having very different structures or containing atoms of different chemical species. An alternative explanation was given by us in Ref. 11 and supported by calculations showing a nice agreement with the experimentally measured band structure: the two proximal bands would appear due to the spin-orbit (SO) splitting (Rashba effect) of a one-dimensional band associated with the gold chains. This model has received some experimental support recently. Measurements of the plasmon dispersion in the Si(557)-Au surface by Nagao *et al.*¹⁷ point to the importance of the SO interaction in this system. Furthermore, very recent photoemission measurements in the Si(553)-Au surface, which shows a band structure very similar to the Si(557)-Au reconstruction,¹ seem to confirm that the origin of the two proximal bands is the SO splitting.¹⁸ However, the authors of this reference arrived to this conclusion based on the observed pattern of avoided crossings in the band structure. This indirect method was used by Barke *et al.*¹⁸ since the requirements of energy and angle resolution are difficult to combine with the low count rate imposed by spin detection. Thus, the band structure of the Si(557)-Au surface is still a matter of certain debate that needs further experimental and theoretical work to be fully understood.

Another interesting observation on the Si(557)-Au system was recently made by Ahn *et al.*⁸ using variable temperature scanning tunneling microscopy (STM). The structure located at the edge of every step in the Si(557)-Au surface was observed to undergo a periodicity doubling consistent with a Peierls-type instability²³ as the temperature was decreased to ~ 78 K. These temperature dependent STM images were correlated with ARPES measurements. One of the two proximal one-dimensional bands was shown to suffer a metal-insulator transition, while the other band was claimed not to cross E_F (i.e., remain insulating) independently of the temperature.⁸

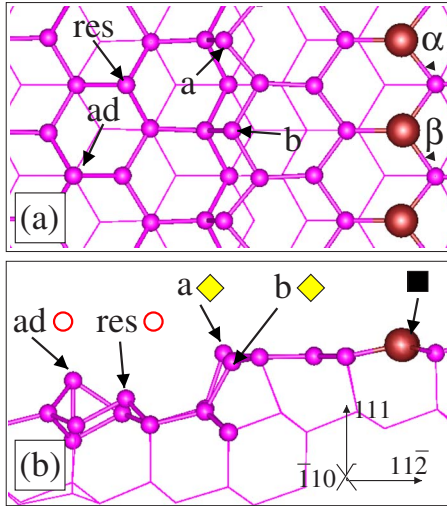


FIG. 1. (Color online) (a) Top and (b) side views of the structure of the Si(557)-Au reconstruction. The larger circles correspond to the gold atoms. The most prominent features of the surface are highlighted: a row of adatoms (*ad*), restatoms (*res*), a buckled step edge with up-edge (*a*) and down-edge (*b*) Si atoms, and a chain of gold atoms with alternating Si-Au-Si bond angles (α and β). The symbols close to each type of atom correspond to those used below in Fig. 4 to indicate the main atomic character of the different surface bands.

This last observation is in contrast with previous^{1,5} ARPES measurements where both bands were found metallic at room temperature. From their results, Ahn *et al.* concluded that at least one of the two proximal bands should be associated with the atoms forming the step edge. This is in clear contrast with our suggestion that the SO splitting is responsible for the appearance of the two proximal bands¹¹ and the recent experimental evidence that seems to support this idea.^{17,18}

The strong interaction between the electronic and atomic degrees of freedom, and the corresponding appearance of structural distortions and accompanying electronic transitions at low temperature, is characteristic of low-dimensional systems and is expected for quasi-one-dimensional surface reconstructions like the one considered here. It has been observed for systems like, for example, the In/Si(111)- 4×1 (Refs. 24–26) and the Si(553)-Au (Refs. 27–29) surfaces. The calculations presented in Ref. 11 provided insight into some of the structural distortions suffered by the Si(557)-Au. The most important one involves the atoms at the step edge. In principle, the silicon atoms forming the step edge are all equivalent and have a dangling bond occupied by one electron. This structure would give rise to a flat electron band with half occupation. This is a quite unstable situation. Thus, the system suffers a distortion in which the step-edge atoms alternate between up and down positions. The dangling bonds corresponding to the up-edge silicon atoms become doubly occupied, whereas those associated with the down-edge atoms are empty. A gap Δ_{step} is opened between occupied and unoccupied step-edge bands.

The stabilization of the step-edge buckling as the temperature is decreased provides a plausible explanation for the

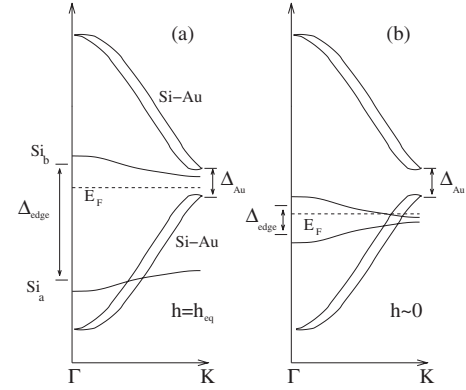


FIG. 2. Schematic picture of a plausible model, based on the theoretical band structure, of the metal-insulator transition in the Si(557)-Au surface controlled by the buckling of the step edge. Panel (a) shows the insulator situation for the equilibrium, low-temperature, structure. The Si-Au label indicates the spin-split gold bands with a gap Δ_{Au} due to the periodicity doubling caused by the row of silicon adatoms in the terrace. The buckling of the step edge opens a gap Δ_{edge} , leaving an occupied band coming from the up-edge atoms (Si_a) and an unoccupied band coming from the down-edge atoms (Si_b). The position of the Fermi level is indicated by E_F , and $h = |h_a - h_b|$ is the height difference between the atoms *a* and *b* in the step edge. Panel (b) shows the metallic situation for $h \sim 0$. If the buckling of the step edge takes place through a displacive distortion, $h \sim 0$ corresponds to the high-temperature undistorted configuration. If the transition takes place through an order-disorder transition, configurations close to $h \sim 0$ will have a larger weight as the temperature is increased.

Peierls-type transition observed by Ahn *et al.*⁸ In Ref. 11, we proposed that this could happen by the freezing of the dynamical fluctuations of the step edge, in analogy with the accepted model to explain the $3 \times 3 \rightarrow \sqrt{3} \times \sqrt{3}$ transition observed with STM in Sn/Ge(111).³⁰ A similar mechanism has been recently proposed for the In/Si(111)- $4 \times 1 \rightarrow 8 \times 2$ transition,³¹ although this identification is the subject of some controversy.^{32–34}

The situation presented so far raises questions about the relation between the Peierls-type transition of the step edge and the metal-insulator transition observed in the ARPES experiments. According to the existing theoretical model,¹¹ none of the two dispersive one-dimensional bands in the surface is associated with the step edge and, therefore, these bands should remain basically unaltered by the distortion of the step edge. If this is the case, what would be the relation between the experimentally observed structural and electronic transitions? A possible connection was outlined in Ref. 11, and will be presented with more detail in the present paper. The main idea for this scenario of the metal-insulator transition is the following (see Fig. 2 below): the position of the Fermi level is controlled by the size of the band gap at the step edge Δ_{step} which, in turn, is determined by the degree of buckling of the step edge. Depending on the relative energy positions of the gold-derived and step-edge bands, a change in size of the Δ_{step} gap can drive the system from insulator to metallic.

The theoretical model presented above has been strongly criticized by Yeom *et al.*¹³ in a recent experimental paper

using spatially resolved scanning tunneling spectroscopy (STS) measurements. According to Yeom *et al.*, the existing structural model^{10,11} of the Si(557)-Au surface and the band structure that is derived from it fails to reproduce the main characteristics of their STS data either at low or room temperature. Furthermore, they claim that the observation of the opening of a symmetric gap at the step edge is inconsistent with the theoretical description of the surface given in Refs. 10 and 11.

In this paper, we revisit the problem of the Si(557)-Au surface using DFT calculations. We use a more complete basis set than in our previous work¹¹ and, therefore, the relaxed structures and the energy barriers are expected to be more reliable. We focus on the coupling between the atomic and electronic degrees of freedom and address the most recent STM and STS results for the Si(557)-Au surface. In particular, we consider in detail the studies performed at room temperature by Krawiec *et al.*¹⁴ and the variable temperature STS results of Yeom *et al.*¹³ Our predictions are in qualitative agreement with the results presented by these authors, giving further support to the current structural model of the Si(557)-Au surface^{6,10} and the predictions of the DFT calculations for its electronic band structure.¹¹ We also consider in detail the energetics and variation of the band structure as a function of the buckling of the step edge and its implications to explain the observed metal-insulator transition.⁸ Finally, we present the results of a first-principles molecular dynamics simulation of several picoseconds. We find that the step-edge atoms indeed fluctuate at room temperature. The dynamics associated with other modes is also observed. Particularly apparent are the oscillations of the height of the restatoms and adatoms, which induce important changes in the Si–Au–Si bond angles along the gold chains. This is important for the electronic band structure, since these angles are the main parameters that control the size of the band gap Δ_{Au} that opens in the spin-split one-dimensional band associated with the gold chains.

II. COMPUTATIONAL METHOD

Our density functional calculations are performed using the SIESTA code.^{35–37} We have used here the local density approximation (LDA) to the DFT,^{38–40} Troullier-Martins pseudopotentials,⁴¹ and a 5×2 k -point sampling. The fineness of the real-space grid used to compute the Hartree and exchange-correlation contributions to the total energy and Hamiltonian matrix elements was equivalent to a 100 Ry plane-wave cutoff. This guarantees the convergence of the total energy, for a given basis set, within ~ 50 meV/Au (~ 0.7 meV/Å²). Several surface bands are much more dispersive along the step-edge direction. Therefore, we have checked the convergence of our band structures using a 16×2 k -point sampling, which is denser along this direction. We have used a double- ζ polarized (DZP) basis set of numerical atomic orbitals obtained from the solution of the atomic pseudopotential at slightly excited energies.^{35,36,42,43} This basis set includes two different functions (i.e., two different radial shapes) to represent the $3s$ and $3p$ orbitals of Si, the $5d$ and $6s$ orbitals of Au, and the $1s$ orbital of H. In

addition, it contains a polarization shell with d symmetry for Si and p symmetry for Au and H. The cutoff radii of the orbitals are defined using an *energy shift*^{36,43} of 200 meV. These radii are 5.3, 6.4, and 6.4 a.u. for the s , p , and d orbitals of Si, 6.2, 6.2, and 4.5 a.u. in the case of Au, and 5.1 a.u. for the s and p states of H. We notice that this basis set is more accurate than the double- ζ (DZ) basis used in our previous study of the energetics of the Si(557)-Au.¹¹ In Ref. 43, it was shown that, for a large variety of systems, the DZP basis sets were able to provide results (for the geometry and energetics) comparable to those of reasonably well-converged plane-wave calculations. Indeed, in our recent study of the Si(111)-(5 \times 2)-Au (Ref. 44) reconstruction we found that, with calculational parameters similar to those used here, our SIESTA results are in very good agreement with those obtained with well-converged plane-wave calculations (see, in particular, Table II in Ref. 44). We have also applied a similar methodology to the study of the Si(553)-Au (Refs. 45 and 46) and In-Si(111)-4 \times 1 (Ref. 47) surface reconstructions.

In the present calculation, we do not include the spin-orbit interaction. The SO coupling is necessary to recover the two proximal one-dimensional dispersive bands observed in the experimental band structure.¹¹ However, the SO splitting should not play a crucial role in determining the structural properties and energetics of the system. Without the SO interaction, we obtain only one gold-derived dispersive band at the average energy. In order to compare with the experiment, one should always keep in mind the existence of a SO splitting of this band by a few tenths of eV (~ 300 meV at E_F).

We modeled the surface using a slab consisting of three silicon bilayers (one at the surface and two underlying silicon bilayers) plus an additional layer of hydrogen atoms to saturate the silicon atoms in the bottom of the slab. During the structural relaxations, the positions of the silicon atoms in the bottom layer were kept at the bulk ideal positions. The corresponding hydrogen atoms were also kept fixed. Unless otherwise stated, all other degrees of freedom were optimized until all the components of the residual forces were smaller than 0.04 eV/Å. To avoid artificial stresses, the lateral lattice parameter was adjusted to the theoretical bulk value calculated using similar approximations to those utilized in the slab calculations, i.e., the same basis set and grid cutoff, and a consistent k sampling. The calculated lattice parameter of silicon with our DZP basis is 5.42 Å, to be compared with the experimental value of 5.43 Å.

In our calculations, we study in detail the influence of the step-edge buckling in the electronic structure and simulated STM and STS images. We do this using constrained structural relaxations in which a given buckling is fixed in the step edge, while the rest of the degrees of freedom of the system are optimized. However, we have also performed molecular dynamics (MD) simulations. These simulations are important to check whether a well-defined fluctuation of the step edge actually takes place and how it is coupled to other vibrational modes in the surface. For the MD simulation, the computational details are identical to those described above, with the exception of the basis set for silicon: we have used a DZ basis. This was necessary to accelerate the calculations and allow performing simulations of several picoseconds.

The Verlett algorithm was used for the integration of the equations of movement⁴⁸ and the time step was chosen to be 1 fs. Finally, the simulations of the STM and STS images were performed using Tersoff-Hamann theory.⁴⁹

III. RESULTS

A. Step-edge buckling and the metal-insulator transition

The interpretation of the electronic structure of the Si(557)-Au surface based on the DFT calculations^{10,11} leaves open the question about the nature of the connection between the structural transition of the step edge observed by STM and the metal-insulator transition observed by ARPES.⁸ According to these calculations, the two dispersive one-dimensional bands that dominate the ARPES spectra are spin-split bands coming from the Au-Si-Au chains in the terraces (Si-Au bands hereafter). The gold chains are spatially well separated from the step edge (see the structure in Fig. 1) and, therefore, the Si-Au bands should not be affected by a Peierls-type distortion of the step edge. This point has been recently stressed by Yeom *et al.*¹³

However, we claim that the theoretical band structure of Si(557)-Au surface contains all the necessary ingredients to justify the appearance of a metal-insulator transition driven by the step-edge distortion. Figure 2 schematically presents the main ingredients and clarifies a possible mechanism for such transition. These are as follows.

(i) Due to the periodicity doubling imposed by the presence of a neighboring row of silicon adatoms, a band gap Δ_{Au} appears in the Si-Au bands at the Brillouin zone boundary.

(ii) The buckling opens a gap between occupied and unoccupied levels at the step edge Δ_{step} , and the size of this gap depends on the strength of the step-edge distortion, i.e., is a function of $|h|=|h_a-h_b|$ the difference between the height of up- and down-edge atoms along the step edge (see Fig. 1).

(iii) The Fermi level position is controlled by the relative position of the upper step-edge band (this band is unoccupied at low temperature, its energy being dependent on the step-edge distortion) and the top of the occupied Si-Au bands.

(iv) If the alignment of the Si-Au and step-edge bands is appropriate, a change in size of Δ_{step} will drive a metal-insulator transition [compare Figs. 2(a) and 2(b)].

If the band structure of Si(557)-Au is qualitatively similar to that in Fig. 2 (and we will show that this is the case), a displacivelike transition of the step edge between a distorted ($h=h_{\text{eq}}$) low-temperature and an undistorted ($h\sim 0$) high-temperature configuration will be accompanied by a transition from an insulator to a metallic state as the temperature is raised, in agreement with the experimental observations.⁸ Thus, the connection between the step-edge distortion and the metal-insulator transition of the Si-Au bands has been established: the metallic and/or insulating character is determined by the position of E_F , the size of Δ_{step} controls E_F , and Δ_{step} is determined by the strength of the distortion h .

In Ref. 11, we pointed out the possibility that the step-edge transition could be order-disorder, with the system fluctuating between two equivalent equilibrium configurations at room temperature. Such an order-disorder transition would

make difficult the direct application of the model of the metal-insulator transition sketched in Fig. 2. However, this assignment was only an attempt to draw an analogy with the “dynamical fluctuation” model accepted for the Sn/Ge(111) and related surfaces.³⁰ The displacive or order-disorder character of the phase transition depends on the ratio between the energy gain associated with the local distortion and interaction between distortions created in nearby sites, and how such interaction decays with distance. As a function of these parameters, there is a continuous crossover between both types of phase transitions.⁵⁰⁻⁵² Unfortunately, the information necessary to fully characterize the step-edge structural transition in the Si(557)-Au cannot be obtained from *ab initio* calculations using small unit cells and thus is beyond the scope of the present study. We notice, however, that the time spent by the system in configurations with small values of h (slightly distorted step edge), and thus metallic, increases as the temperature is raised even in the case of an order-disorder transition.

In Fig. 1 of Ref. 11, we can find the LDA band structure of the Si(557)-Au surface in its equilibrium configuration calculated with and without the SO interaction. The sole difference between both band structures is the splitting of the Si-Au bands. Very similar band structures are found using the generalized gradient approximation to DFT. The surface is metallic. However, the metallicity stems from the small overlap between the upper step-edge band and the occupied Si-Au bands. If the step-edge band is lifted by ~ 0.1 eV, the surface becomes insulating, in agreement with some of the most recent experimental observations.^{8,12,13} Taking into account the use of LDA, and the very different origin of both bands, the existence of inaccuracies of a few hundreds of meV in their relative positions is not surprising. In fact, the limitations of LDA to describe the excitation spectra associated with the dangling bonds in silicon surfaces have been studied in detail by several authors. For example, in the case of the Si(001)-(2×1) (Ref. 53) and Si(111)-(2×1) (Ref. 54), the gap between the occupied and unoccupied surface bands is widened ~ 0.5 eV using the GW approximation for the electron self-energy. The unoccupied surface bands appear shifted to higher energies with respect to the occupied surface and bulk states. The GW approximation provides a better description of the exchange and correlation effects than the LDA. In particular, the use of a nonlocal self-energy allows for a better description of the electronic exchange which is crucial for an appropriate treatment of the relatively localized silicon dangling bonds. The origin of the step-edge bands in Si(557)-Au is very similar to, for example, the surface bands associated with the tilted dimers in the Si(001)-(2×1) surface. We can exploit this analogy in order to understand the possible effect of the GW approximation in the electronic structure of the Si(557)-Au surface. The distorted low-temperature structure of the step edge is similar to the asymmetric dimer model of the Si(001)-(2×1) surface, whereas the undistorted step edge can be considered as equivalent to the symmetric dimer model. In accordance with this analogy, the buckled structure presents a band gap in the step-edge band even within the LDA approximation. This band gap becomes zero as the distortion of the step edge disappears. Thus, from what is known for the Si(001)-(2

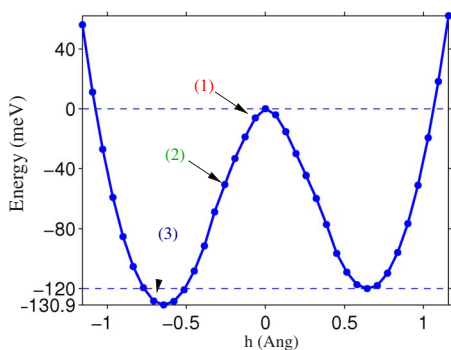


FIG. 3. (Color online) Total energy calculated with a DZP basis set as function of the relative height (h) of the step-edge atoms. Notice the slight asymmetry of the curve corresponding to the inequivalency of the two step-edge positions due to the presence of a row of adatoms in the *same* terrace. Three configurations, corresponding to different sizes of the step-edge buckling, are selected: configuration (1) corresponds to a negligible buckling, (2) to an intermediate value, and (3) is close to the optimum strength of the distortion. The local density of states and band structure of these configurations are analyzed and presented below in Figs. 4–6.

×1) surface, for the distorted structure we can expect a shift of the unoccupied step-edge band to higher energies by a few tenths of eV using a description of the exchange and correlation beyond DFT-LDA. The undistorted step edge, however, should remain metallic, with a negligible step-edge band gap. This would render the low-temperature structure of the Si(557)-Au surface insulating, corresponding to the scheme shown Fig. 2(a), in agreement with recent experimental observations, and would explain the observation of an insulator-to-metal transition as the buckling of the step edge decreases. Of course, this suggestion should be verified by performing the actual calculations. Unfortunately, most theoretical methods beyond DFT become rapidly inapplicable to the large unit cells necessary to simulate the present system, containing close to 100 atoms, and we will restrict to LDA calculation in the present paper.

In the following sections, we will analyze the changes of the electronic structure as a function of the step-edge distortion. We will see that these results support the plausibility of the model proposed in Fig. 2 and reproduce most of the features of the recent STM and STS experiments.^{13–15}

B. Step-edge buckling: Energetics and band structure

Figure 3 presents the total energy as a function of the step-edge buckling h . With the DZP basis set used here, the buckling distortion is favorable by at least 120 meV. This is four times larger than the ~ 30 meV obtained with the less complete DZ basis set used in Ref. 11. The value of the distortion at equilibrium h_{eq} is 0.65 \AA , also larger than the 0.4 \AA obtained with a DZ basis. A value of h corresponds to a given up-down configuration along the step edge, while $-h$ corresponds to the reverse arrangement. Therefore, we find equilibrium configurations at h_{eq} and $-h_{eq}$. Notice, however, that one of them is slightly more stable (by 11 meV). This asymmetry is due to the different registry of the two step-

edge atoms with respect to the silicon adatoms on the *same* terrace, which are located $\sim 12 \text{ \AA}$ away. Both step-edge positions are equivalent with respect to the closest adatom row, located $\sim 7 \text{ \AA}$ away from the step edge.

Our results for the energetics of the buckling distortion seem to be more consistent with the experimental observation. The previously reported value of 30 meV had been claimed too small to explain the observed stabilization of the step-edge buckling at temperatures of 78 K.¹³ However, we should stress two points here. On the one hand, present theoretical methods⁵⁵ are probably not accurate enough to reliably estimate the small energy associated with the step-edge distortion in the Si(557)-Au surface. We can expect considerable inaccuracies associated with the use of approximate DFT functionals. On the other hand, this quantity is not sufficient to determine the apparent transition temperature in a real system with defects [see, for example, the “vacancies” in the step edge and the adatom row of the Si(557)-Au surface in Fig. 3 of Ref. 8]. It has been shown⁵⁶ that the presence of defects can stabilize locally a reconstruction well above the phase transition temperature of the system. Given the very small energy differences between different reconstructions of the surface, the presence of defects is usually a very strong perturbation. Defects typically pin a particular surface configuration in their neighborhood. Therefore, the temperature at which a single step-edge configuration starts to be resolved in the STM images will depend critically on the type and the density of defects present on the Si(557)-Au surface. For example, the room-temperature STM images of Krawiec *et al.*¹⁴ resolve the step-edge modulation in clean sections of the step edge of at least 10 nm limited by defects. The stabilization of the periodicity doubling of the step edge at room temperature nearby defects has also been observed by other authors.^{5,13} Since the appearance of a relatively large density of defects seems unavoidable in this surface, the estimation of the transition temperature from calculations of the “perfect” surface can be questionable.

In Fig. 3, we have selected three different configurations corresponding to (1) a very small step-edge distortion ($h=0.06 \text{ \AA}$), (2) an intermediate value ($h=0.25 \text{ \AA}$), and (3) close to the equilibrium configuration ($h=0.70 \text{ \AA}$). The corresponding band structures along the direction of the step edge are plotted in Fig. 4. The different surface bands are marked according to their main atomic character. Solid (blue) squares indicate the Si-Au bands, open (red) circles mark those bands associated with the adatoms and restatoms, and (yellow) diamonds correspond to the bands coming from the step-edge atoms. We see that only those bands that come from the step-edge atoms are modified as we change the strength of the buckling distortion. The step-edge gap Δ_{edge} is strongly reduced as the size of the distortion diminishes. The difference between the average position of the step-edge bands is 0.9 eV for configuration (3), but only 0.2 eV for structure (1). The occupied step-edge band, associated with the up-edge atoms, is always very flat (dispersion smaller than 0.1 eV), and its position evolves from -0.8 eV (below E_F) in (3) to -0.17 eV in (1). The behavior of the “unoccupied” step-edge band, coming from the down-edge atoms, is somewhat more complex. For configurations (1) and (2), this band is pinned at E_F , whereas its average position in (3) is

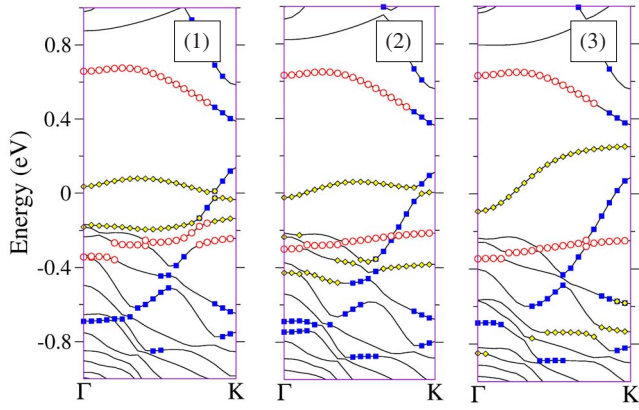


FIG. 4. (Color online) Band structures of the three configurations selected in Fig. 3. The different symbols (also indicated in Fig. 1) indicate the main atomic character of the different surface bands: filled squares for bands coming from the gold atoms and their neighboring silicon atoms, diamonds for the step-edge atoms, and open circles for the adatoms and restatoms. In the case of the step edge, the (partially) unoccupied band corresponds to the down-edge atoms (Si_b in Fig. 1), while the fully occupied one comes from the up-edge atoms (Si_a). As expected, the band coming from the adatoms is unoccupied, while the restatom band is fully occupied. Energies are referred to the Fermi level.

~ 0.15 eV above E_F . This is in agreement with our proposal for the metal-insulator transition. However, while the dispersion of the band is very small for configurations (1) and (2), for structure (3) it becomes ~ 0.35 eV. This small occupation is probably an artifact of the DFT-LDA calculation as we pointed out in the previous section. As commented there, in relation with the GW results for the asymmetric dimer reconstruction of the Si(001)-(2 \times 1) surface,⁵⁴ a better treatment of electron exchange and correlation is likely to shift this band to higher energies.

As expected, when the step-edge buckling h is reduced, the down-edge atom band is shifted to lower energies and this shift is accompanied by a charge transfer from the Si-Au band to the step edge. However, we can expect this charging to be moderate and the occupation of this band should always remain relatively small. Indeed, going from configuration (3) to (2) shifts down the center of the band ~ 0.2 eV, while going from configuration (2) to (1) this band does not considerably move with respect to the other surface bands. As a consequence, the closing of the step-edge gap implies a larger movement of the occupied step-edge band, which moves ~ 0.6 eV to higher energies. This asymmetric closing of the step-edge gap is a distinct feature of our theoretical model of the Si(557)-Au and has been claimed to be in disagreement with the experimental evidence.¹³ In fact, the observed gap closing in the dI/dV spectra on the step edge reported in Ref. 13 is apparently symmetric. However, if we examine these data in detail, we can find several features that are in qualitative agreement with the predictions of our model. For example, the differences between the low- and room-temperature data are more significant for the occupied part of the spectrum. In particular, a strong peak located at ~ 0.7 eV below E_F in the low-temperature spectrum disap-

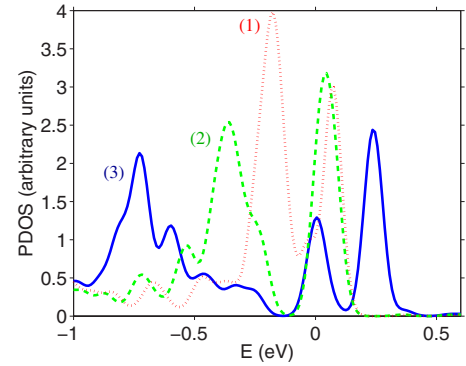


FIG. 5. (Color online) Density of states projected onto the step-edge atoms for the three configurations selected in Fig. 3. The energies are referred to the Fermi level.

pears at room temperature. This energy coincides nicely with the position of the occupied step-edge band in our low-temperature configuration (3).

C. Simulated STM and STS images

In Fig. 5, we show the projected density of states (PDOS) onto the step-edge atoms as a function of the energy. This can be directly compared with the dI/dV spectra measured on the step edge and presented in Fig. 4 of Ref. 13. The solid (blue) curve presents the PDOS for our low-temperature configuration (3). Below E_F , we find the main peak at -0.71 eV, in good agreement with the experiment. We also find the contribution coming from the bulk states up to ~ 0.2 eV below E_F . At higher energies, we find a gap in the PDOS. Two peaks, at E_F and 0.24 eV above E_F , appear due to the dispersion of the down-edge atom band. Besides the small occupation of the down-edge atom band, which is not observed in the experiment and gives rise to a peak at E_F , the main peak at -0.71 eV and the gap extending down to -0.2 eV agree with the observed low-temperature dI/dV spectra. For configurations (2) and (1), the main occupied peak shifts to higher energies and, as a consequence, the gap in the PDOS is considerably reduced. Although the changes are more modest above E_F than below E_F , we also observe a shift to lower energies of the main unoccupied peak that becomes pinned at E_F . Configurations like (1) and (2) are only available at high-temperature. If the structural transition is purely displacive, then the high-temperature spectra can be identified with the curve for structure (1). However, in an order-disorder transition the high-temperature dI/dV corresponds to an average of the curves obtained for different structures. Since STM is a local probe, such an average has to reflect the dynamics of the fluctuation process, not just a thermal average. Thus, we can expect structures similar to configuration (1) to have a strong weight in this average.

Thus, we have seen that our model can explain some features of the dI/dV obtained on the step edge of the Si(557)-Au surface. It is also interesting to note that these experiments mainly reflect the changes in the atomic and electronic structure of the step edge. The curves in Fig. 5 do not contain features directly related with the Si-Au bands that dominate the photoemission. In our model, the metal-

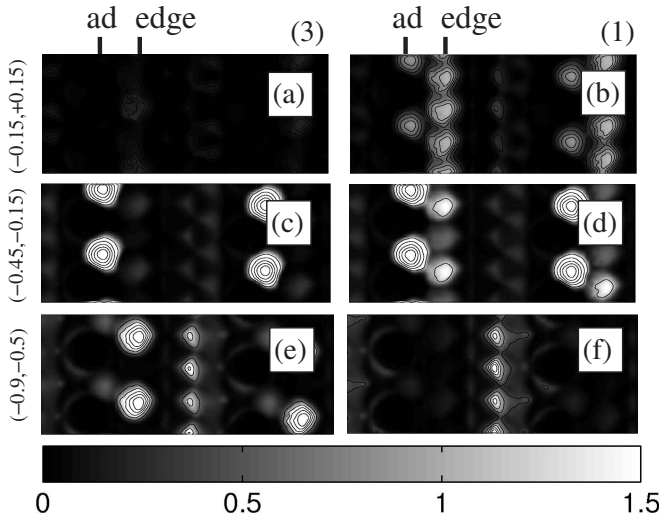


FIG. 6. Calculated maps of the density of states as a function of the energy for the Si(557)-Au surface. Panels (a), (c), and (e) show the result for a buckled step edge [corresponding to configuration (3) in Fig. 3]. Panels (b), (d), and (f) correspond to a negligible step-edge buckling [using configuration (1) in Fig. 3]. The density of states is integrated in various energy ranges: from -0.9 to -0.5 eV [panels (e) and (f)], from -0.45 to -0.15 eV [panels (c) and (d)], and from -0.15 to 0.15 eV [panels (a) and (b)], with zero corresponding to the Fermi energy. The locations of one adatom row and one step edge are indicated by “ad” and “edge,” respectively. The dimension of each image is $\sim 3.3 \times 1.5$ nm². The used gray scale (arbitrary units) is indicated.

insulator transition of the Si-Au bands is a consequence of the change in position of the down-edge atom band, from above E_F to be pinned at E_F .

Figure 6 shows the calculated maps of the local density of states (LDOS). These maps can be compared with the dI/dV maps in Fig. 3 of Ref. 13. The LDOS maps of the surface were produced mimicking the experimental procedure: First, we find the “tip height” $Z_{tip}(x, y)$ corresponding to a constant current image at a positive bias of $+2.0$ V (the results of the LDOS maps do not significantly depend on this voltage),

$$I = \int_{E_F}^{E_F+V} d\epsilon \rho(x, y, Z_{tip}(x, y), \epsilon) = \text{const}, \quad (1)$$

where $\rho(\mathbf{r}, \epsilon)$ is the local density of states calculated for the energy ϵ at point \mathbf{r} . We then plot the local density of states on the surface $Z_{tip}(x, y)$ integrated in small energy intervals ΔV as an approximation to the measured dI/dV maps,

$$\text{LDOS}(x, y, V) = \int_{E_F+V-\Delta V/2}^{E_F+V+\Delta V/2} d\epsilon \rho(x, y, Z_{tip}(x, y), \epsilon). \quad (2)$$

The size of the intervals ΔV depends on the fineness of the k sampling and the dispersion of the bands. For typical calculational parameters, ΔV cannot be too small. In our case, we have divided the range between $+0.15$ and -0.9 eV in two intervals of 0.3 eV and one of 0.4 eV, which correspond to the main position of the different surface bands in the low-temperature structure.

In agreement with the experimental results, the data in Fig. 6 are dominated by features coming from the step edge and the adatom-restatom row, that correspond, respectively, to the α and β chains of Ref. 13. At low temperatures and small voltage [panels (a) and (c)], the LDOS maps are dominated by the signal coming from the restatoms at ~ 0.3 eV below E_F . We can only see extremely faint features associated with the step edge and the Si-Au chain in the middle of the terrace. We need to go to lower energies, around -0.8 eV, to observe a strong feature associated with the step edge [panel (e)]. We can also see an increase in the intensity of the signal coming from the middle of the terrace. This corresponds to a relatively flat band associated with one of the three silicon atoms bonded to each gold atom. This surface resonance is not clearly marked in Fig. 4 but can be found in the band structures presented in Refs. 10 and 11. The bonds between gold and the other two silicon atoms generate the dispersive Si-Au band seen in photoemission that, however, only produces a very weak signal in the STM and STS images. At high temperature [panels (b), (d), and (f)], the situation changes as seen in the experiment: the step edge becomes clearly visible at low voltages.

Recently, Krawiec *et al.*¹⁴ have reported an interesting experimental result. While the topography of one of the two atomic rows that characterize the STM images of the Si(557)-Au depends on the sign of the applied bias voltage, it remains unchanged for the other wire. They suggest that the different behavior is an indication that both wires are made of different materials, gold and silicon. However, we claim that this experimental observation can be perfectly understood using the present structural model where the two prominent chains are assigned to the step edge and the adatom row, respectively. The step edge shows a reverse corrugation as function of the bias polarity, whereas this does not happen for the adatom row. The silicon adatoms are ~ 1.3 Å higher than the other atoms in the surface layer, except for the restatoms that only lie ~ 0.8 Å below. Although the adatoms produce more pronounced features at positive bias and the restatoms at negative bias, for scan lines taken along the rows of adatoms the atomic topography dominates over the electronic effects. Therefore, the STM images show maxima at the adatom positions irrespective of the sign of the applied voltage. This can be seen in Fig. 7(d). The corrugation is larger for empty states and the data are in good qualitative agreement with the images of Krawiec *et al.* (see the data for chain D in Fig. 3 of Ref. 14). In contrast, the electronic effects dominate for the scans taken along the buckled step edge, and the topography can show a pronounced bias dependence. This is shown in Fig. 7(c), again in good qualitative agreement with the data for chain C in Ref. 14 (see Figs. 3 and 5 in that reference). Notice that we use our low-temperature structure (with fully developed step-edge buckling) to generate the images in Fig. 7. Although the experiments of Krawiec *et al.* are made at room temperature, the use of this geometry is justified by the fact that these authors concentrate in sections of the step edge of a few nanometers bounded by defects. The presence of defects stabilizes the step-edge distortion up to room temperature for these relatively short chains, as was mentioned above.

It is interesting to note that one of the criticisms of Yeom *et al.*¹³ toward the low-temperature structure proposed by

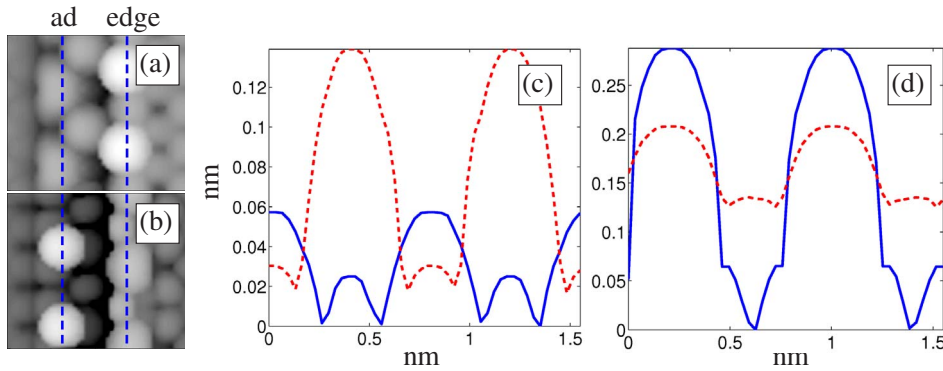


FIG. 7. (Color online) Simulated STM images with bias of (a) -1.0 V and (b) $+0.6$ V. Plots in (c) and (d) show the calculated topography along the step edge (“edge”) and the row of adatoms (“ad”), respectively. Solid lines are for empty states (positive bias) and dashed lines for occupied states (negative bias). The used scan lines are indicated by dotted lines in (a) and (b).

Robinson *et al.*⁶ and Sánchez-Portal *et al.*^{10,11} was based on the predictions, using such structural model, of the appearance of a step-edge modulation for both empty and occupied states.¹¹ According to Yeom *et al.*, such modulation could only be observed for empty states. However, this is in disagreement with the results presented in Ref. 14. Of course, one could argue that the step-edge modulation observed in the presence of defects is different from the modulation stabilized at low temperature. However, most experiments to date have been performed on samples with a considerable concentration of defects and the observations of Krawiec *et al.* seem to agree with the predictions from theory. Thus, it is quite tempting to identify the distortions observed at low temperature and in the presence of defects. Furthermore, the simulated STM images seem to reproduce the change in the relative intensity of the step edge and the adatom row as a function of voltage. In Figs. 7(a) and 7(b), we can see that for a voltage of -1.0 V the step edge is more intense than the adatoms, whereas for $+0.6$ V the situation is reversed. This is in agreement with the STM images shown in Fig. 2 of Ref. 14, although might be strongly dependent on the tunneling conditions (e.g., this change is not so clear in the data in Fig. 2 of Ref. 13).

The agreement of the simulations in Fig. 7 with experiment is qualitative. From a more quantitative point of view, there are some discrepancies: (i) the calculated corrugations are too large and (ii) the step edge shows a larger corrugation for occupied states than for empty states, which is not ob-

served in the experiment.¹⁴ We should point here that we are using the simple Tersoff-Hamann⁴⁹ theory for our simulations. In this theory, the STM images are obtained from the local density of states of the surface according to Eq. (1) and all the effects induced by the tip are neglected. The observed discrepancies are probably related to the simple theoretical treatment and the use of a basis set of confined atomic orbitals in our calculations.^{35,43} This basis set is numerically very efficient. However, due to the short cutoff radii of the orbitals, it is not adequate to simulate the smooth decay of the wave functions toward the vacuum and tends to emphasize the structural corrugation over the electronic effects and, in general, leads to an overestimation of the surface corrugation. This also explains, at least partially, the second discrepancy. The empty state images might also be influenced by the difficulties of the DFT calculations to properly describe the excited states.

D. Molecular dynamics simulations

Our MD simulations have been performed using a DZ basis set, similar to that used in previous studies of the structural properties of the Si(557)-Au surface.^{7,10,11} With this basis set, we can perform simulations of several picoseconds. Although less complete than the DZP basis set used in the previous sections, the structural and electronic properties obtained with the DZ basis set are very similar to those described above. Figure 8 shows the behavior of several de-

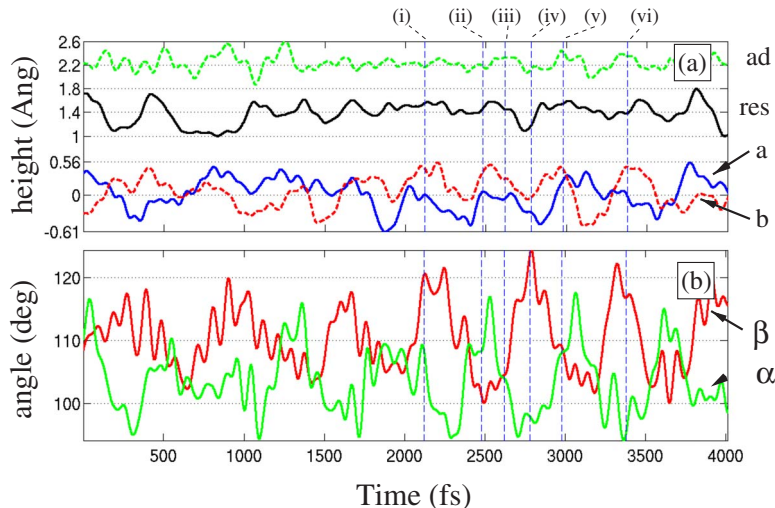


FIG. 8. (Color online) Last 4 ps of a molecular dynamics simulation of the Si(557)-Au reconstruction performed at a temperature of ~ 300 K. A DZ basis set was used for this calculation and the total simulation time is 8 ps. Panel (a) displays the height of different atoms as a function of time (see also Fig. 1): adatom (*ad*, green dashed line), restatom (*res*, solid black line), and the step-edge atoms (*a*, solid blue line and *b*, dashed red line). The two inequivalent Si-Au-Si bond angles (α and β) are presented in panel (b). The vertical lines mark the instantaneous configurations for which the band structures are shown in Fig. 9.

degrees of freedom during the last 4 ps of one of our MD simulations. The total simulation time is 8 ps (8000 time steps). The temperature of the system oscillates around 300 K after a thermalization time of ~ 1 ps. Our simulation cell contains one unit cell of the Si(557)-Au surface. With this “small” cell, we cannot obtain a realistic picture of the structural transition in the surface. Furthermore, we have seen that the use of a DZ basis set causes a severe underestimation of the energy barrier between the two step-edge equilibrium configurations (the barrier is ~ 30 meV and the equilibrium step-edge distortion $h_{eq} \sim 0.4$ Å). However, the MD simulations are a very important tool to understand the coupling between different vibrational modes and between the atomic and electronic degrees of freedom. In particular, we want to check if a well-defined fluctuation of the step edge exists at high temperatures and how this movement is coupled with other vibrational modes. We also study the effect in the electronic structure of atomic movements that can be excited at reasonable temperatures and are different from the step-edge fluctuation studied in detail above.

Figure 8 shows a clear oscillation of the step edge, the atoms changing their relative positions and residing for intervals of less than 1 ps in a given up-down configuration. We can also observe that the system spends a considerable amount of time in configurations where the step-edge distortion h is small (corresponding to a small step-edge gap Δ_{edge}). Besides the step edge, other degrees of freedom show strong fluctuations in spite of the moderate temperature. Particularly remarkable are the cases of the restatom (marked with *res* in Fig. 8, see also Fig. 1), the Si-Au-Si bond angles (α and β) and, to less extent, the adatom (*ad*). As a consequence, the corresponding energy levels also exhibit a considerable movement during the simulation. The case of the step-edge bands has been studied in detail in the previous sections. The bands associated with the restatom and the adatom oscillate with an amplitude of up to ~ 0.2 eV. This can be easily appreciated for the adatom band (flat band ~ 0.5 eV above E_F) in the band structures shown in Fig. 9 corresponding to different snapshots of the simulation. This movement might be one of the reasons why a well-defined restatom state has not been detected in photoemission experiments² on this surface and why the adatom band appears as a relatively broad structure between 0.5 and 1 V (with its maxima at ~ 0.7 V) in recent STS spectra obtained at room temperature.¹⁵ The Si-Au-Si bond angle has an important influence on the Si-Au band that dominates the photoemission of the surface. The presence of a row of adatoms induces a periodicity doubling in the terraces of the surface that is reflected in an alternating Si-Au-Si bond angle and the opening of a gap Δ_{Au} in the dispersive Si-Au band. In the equilibrium configuration, the values of these two angles are 111.6° and 103.7° , respectively, for β and α . In Fig. 8, we see that these values change by $\sim \pm 10^\circ$ along the simulation. Changing the Si-Au-Si bond angles changes the size of the Δ_{Au} gap and thus influences the metallic or insulating character of the instantaneous configurations.

The influence of the coupling between the electronic and atomic degrees of freedom in the band structure is clearly shown in Figs. 9 and 10. We stress that these band structures are calculated with a DZ basis set and, therefore, differ

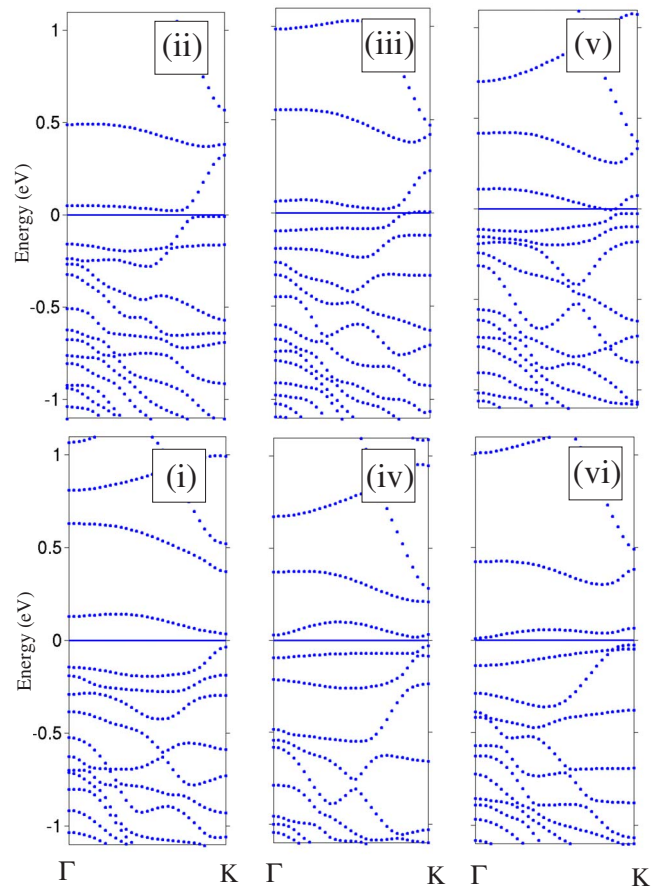


FIG. 9. (Color online) Band structures (calculated with a DZ basis set) corresponding to the snapshots selected in Fig. 8. For configurations (ii), (iii), and (v) (upper panels), the dispersive Si-Au band clearly crosses E_F and the down-edge atom band is pinned at E_F , whereas for configurations (i), (iv), and (vi) (lower panels), the lower branch of the Si-Au band lies below E_F and a tiny gap is developed between this band and the down-edge atom band, i.e., E_F lies within the Si-Au band gap Δ_{Au} .

slightly from those shown in Fig. 4, calculated with a more complete DZP basis. Figure 9 shows the band structure for a few selected structures (indicated in Fig. 8). Figure 10 shows the band structure averaged over the last 3 ps of the simulation (using 151 different configurations, each one taken every 20 fs) and compares it with the band structure for the equilibrium structure. The three band structures in the upper panels of Fig. 9 are clearly metallic: the dispersive Si-Au band crosses E_F and the down-edge atom band is pinned at the Fermi level. For configurations (ii) and (iii), there is an evident reduction of the Si-Au gap Δ_{Au} and a shift in the position of the Si-Au band. This is due to the change of the α and β angles that become quite close or, like in structure (ii), even appear reversed with respect to the equilibrium configuration. For configuration (v), we can also see that the step-edge gap Δ_{edge} is almost closed due to the very similar height of both step-edge atoms. The three lower panels of Fig. 9 show semiconducting band structures where the lower branch of the Si-Au band is fully occupied and a small gap is developed between the down-edge atom band and the Si-Au

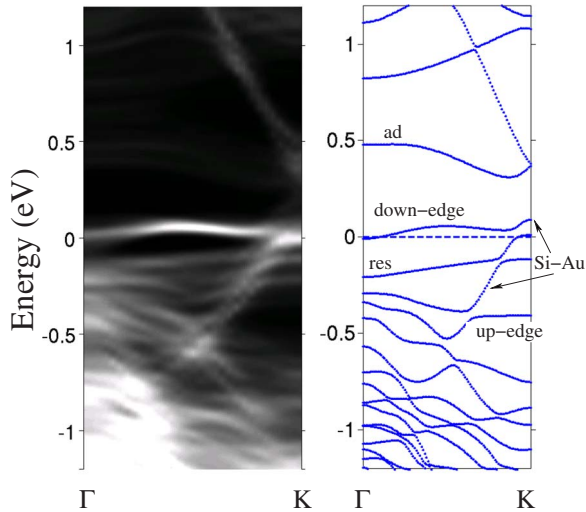


FIG. 10. (Color online) Average band structure (calculated with a DZ basis set) during the last 3 ps of the molecular dynamics simulation of the surface at room temperature shown in Fig. 8. The average is done over 151 configurations (i.e., the band structures are calculated at intervals of 20 fs). The time average is compared with the band structure (also calculated with a DZ basis set) for the equilibrium configuration. Note that the band structure of the right panel corresponds to band structure (3) in Fig. 4. Although both band structures are qualitatively identical, there are small quantitative differences due to the use of different basis sets. In particular, the distortion of the step edge in the equilibrium structure is much smaller when using a DZ basis set (~ 0.4 Å) than a DZP basis set (~ 0.65 Å).

band. As a consequence, the Fermi level lies inside Δ_{Au} . This is particularly clear in the case of configuration (i). In the three configurations, angles α and β differ by a similar or larger amount than in the equilibrium structure and the step edge shows a considerable buckling. This guarantees large values of Δ_{Au} and Δ_{step} and thus insulating configurations of the surface.

The results of the MD simulation indicate that at room temperature we find large fluctuations of Δ_{edge} and Δ_{Au} . According to our model of the electronic structure of the Si(557)-Au surface (schematically summarized in Fig. 2), this implies that at room temperature the system alternates between metallic and insulating configurations. This phenomenon does not depend on the character of the ground state, which will be insulating if the values of Δ_{Au} and Δ_{step} are large enough in the equilibrium configuration.

Interestingly, many bands that can be found in the equilibrium band structure produce very faint signals in the MD average shown in Fig. 10. This is the case, for example, of the adatom band and the occupied (up-edge atom) step-edge band which almost disappear from the average. The restatom band also produces a quite weak and broad structure around -0.2 eV. The most visible features in the MD averaged band structure are (i) the occupied part of the Si-Au band which extends from E_F at the zone boundary down to -0.6 eV where it merges with the bulk bands and the unoccupied branch of the Si-Au band from ~ 0.4 eV above E_F to higher energies, (ii) a quite flat feature coming from the unoccupied step-edge band right above E_F (and thus not visible by pho-

toemission), and (iii) the silicon bulk bands extending around Γ from ~ 0.5 eV below E_F toward lower energies.

IV. CONCLUSIONS

We have presented a detailed discussion of the electronic structure of the Si(557)-Au surface and its coupling to the structural degrees of freedom. Our calculations are based on the structural model for the low-temperature phase of the surface obtained from x-ray diffraction⁶ and density functional calculations.¹⁰ The results are compared with recent experimental information obtained by STM and STS.^{13–15} Our main observations are as follows.

(i) Contrary to the claims of Yeom *et al.*, we have seen that the calculations using the theoretical structural model in Fig. 1 provide nice qualitative agreement with the STM and STS images obtained at low temperatures¹³ and around structural defects that stabilize the step-edge distortion up to room temperature.¹⁴ Together with the successful description of the experimental band structure,¹¹ these results give further support to the current structural model of the Si(557)-Au surface.

(ii) We have shown that the theoretical band structure is close to a metal-insulator transition. The transition is controlled by the relative positions of the dispersive gold-derived and the flat step-edge bands. The latter splits into an occupied and an unoccupied band separated by a gap Δ_{edge} whose size depends on the degree of step-edge buckling, while the former shows a gap Δ_{Au} associated with the presence of a row of adatoms doubling the periodicity along the $[\bar{1}10]$ direction. If Δ_{Au} and Δ_{edge} are large enough, the surface becomes insulating at low temperature (see Fig. 2).

(iii) At low temperature, the step-edge distortion is large and so is Δ_{edge} . As the temperature increases, configurations with a smaller step-edge buckling, and thus with a smaller Δ_{edge} , are available. For sufficiently small values of Δ_{edge} , the system becomes metallic. We argue that this is consistent with the observation of a metal-insulator transition in the Si(557)-Au transition.⁸

(iv) In the present model, the metal-insulator transition is accompanied by an asymmetric (with respect to E_F) closing of the gap. Yeom *et al.* claimed that this is in disagreement with their experimental results. However, we argue that our data provide a simple explanation to the strong changes observed for the occupied states in the dI/dV spectra taken over the step edge by these authors¹³ (a strong peak at -0.71 eV in the low-temperature spectra disappears at higher temperatures).

(v) Our simulated dI/dV maps are in good qualitative agreement with the experimental results at both low and high temperatures. We assume that at room temperature, the system spends a considerable amount of time in structures with a small step-edge distortion. The step edge produces a strong signal that dominates the dI/dV maps of these structures at low voltages; however, in the low-temperature structure the step edge does not produce any distinct feature at small voltages.

(vi) Molecular dynamics simulations of the system show that, besides the fluctuation of the step edge, other vibra-

tional modes are present at room temperature and also have an influence on the electronic structure. In particular, the oscillation of the Si-Au-Si bond angles changes considerably the Δ_{Au} gap. Most configurations with small Δ_{Au} are metallic and contribute efficiently to the metallic character of the surface at room temperature.

(vii) Below E_F , the MD averaged band structure is dominated by a gold-derived band that extends from E_F down to -0.6 eV where it merges with the bulk silicon bands. Other surface bands in the occupied part of the spectrum produce weaker features due to the thermal fluctuations of the structure. This seems to be agreement with the observed photoemission.

The results presented in this work seem to correctly explain many of the experimental observations on the Si(557)-Au surface. However, further theoretical and experimental work is still necessary to understand this surface. In particular, it is necessary to characterize the dynamics of the structural transition⁵² and its relation with the observed metal-insulator transition. Furthermore, the photoemission data of Ahn *et al.*⁸ suggest that only one of the dispersive bands that dominate the spectrum of the Si(557)-Au suffers the metal-insulator transition. This is difficult to explain within the current theoretical model, where the appearance of two bands is due to the spin-orbit splitting. The disorder associated with the presence of defects and the different photoemission matrix elements of the two bands can be behind

this observation and have to be analyzed before drawing further conclusions from this observation. Finally, we have seen that the calculated LDA ground state of the Si(557)-Au is metallic. This is due to the small overlap between the down-edge atom band and the dispersive Si-Au band. We have argued that this failure could be corrected with an improved treatment of the electron exchange and correlation that would provide a better description of the excited electronic states. This is challenging due to the large cell necessary to study the Si(557)-Au surface. However, it would be very interesting to direct future effort along this direction.

ACKNOWLEDGMENTS

We want to thank E. Canadell and A. García for illuminating discussions. This work was supported by the Basque Departamento de Educación and the UPV/EHU (Grant No. 9/UPV 00206.215-13639/2001), the Spanish Ministerio de Educación y Ciencia (Grant No. FIS2004-06490-C3-02), the European Network of Excellence FP6-NoE “NANOQUANTA” (Grant No. 500198-2), and the research contracts “Nanomateriales” and “Nanotron” funded by the Basque Departamento de Industria, Comercio y Turismo within the ETORTEK program and the Departamento para la Innovación y la Sociedad del Conocimiento from the Diputación Foral de Guipuzcoa.

*swbriris@sc.ehu.es

†sqbsapod@sc.ehu.es

- ¹J. N. Crain, J. L. McChesney, F. Zheng, M. C. Gallagher, P. C. Snijders, M. Bissen, C. Gundelach, S. C. Erwin, and F. J. Himpsel, *Phys. Rev. B* **69**, 125401 (2003).
- ²K. N. Altmann, J. N. Crain, A. Kirakosian, J. L. Lin, D. Y. Petrovykh, F. J. Himpsel, and R. Losio, *Phys. Rev. B* **64**, 035406 (2001).
- ³M. Jalochowski, M. Stozak, and R. Zdyb, *Surf. Sci.* **375**, 203 (1997).
- ⁴P. Segovia, D. Purdie, M. Hengsberger, and Y. Baer, *Nature (London)* **402**, 504 (1999).
- ⁵R. Losio, K. N. Altmann, A. Kirakosian, J. L. Lin, D. Y. Petrovykh, and F. J. Himpsel, *Phys. Rev. Lett.* **86**, 4632 (2001).
- ⁶I. K. Robinson, P. A. Bennett, and F. J. Himpsel, *Phys. Rev. Lett.* **88**, 096104 (2002).
- ⁷D. Sánchez-Portal, J. D. Gale, A. García, and R. M. Martin, *Phys. Rev. B* **65**, 081401(R) (2002).
- ⁸J. R. Ahn, H. W. Yeom, H. S. Yoon, and I. W. Lyo, *Phys. Rev. Lett.* **91**, 196403 (2003).
- ⁹M. Schöck, C. Sürgers, and H. v. Löhneysen, *Thin Solid Films* **428**, 11 (2003).
- ¹⁰D. Sánchez-Portal and R. M. Martin, *Surf. Sci.* **532**, 655 (2003).
- ¹¹D. Sánchez-Portal, S. Riikonen, and R. M. Martin, *Phys. Rev. Lett.* **93**, 146803 (2004).
- ¹²H. Okino, R. Hobara, I. Matsuda, T. Kanagawa, S. Hasegawa, J. Okabayashi, S. Toyoda, M. Oshima, and K. Ono, *Phys. Rev. B* **70**, 113404 (2004).

- ¹³H. W. Yeom, J. R. Ahn, H. S. Yoon, I.-W. Lyo, H. Jeong, and S. Jeong, *Phys. Rev. B* **72**, 035323 (2005).
- ¹⁴M. Krawiec, T. Kwapiński, and M. Jalochowski, *Phys. Rev. B* **73**, 075415 (2006).
- ¹⁵M. Schöck, C. Sürgers, and H. v. Löhneysen, *Europhys. Lett.* **74**, 473 (2006).
- ¹⁶J. A. Lipton-Duffin, J. M. MacLeod, and A. B. McLean, *Phys. Rev. B* **73**, 245418 (2006).
- ¹⁷T. Nagao, S. Yaginuma, T. Inaoka, and T. Sakurai, *Phys. Rev. Lett.* **97**, 116802 (2006).
- ¹⁸I. Barke, F. Zheng, T. K. Rugheimer, and F. J. Himpsel, *Phys. Rev. Lett.* **97**, 226405 (2006).
- ¹⁹S. Tomonaga, *Prog. Theor. Phys.* **5**, 544 (1950).
- ²⁰J. M. Luttinger, *J. Math. Phys.* **4**, 1154 (1963).
- ²¹T. Giamarchi, *Quantum Physics in One Dimension* (Clarendon, Oxford, 2004).
- ²²S. C. Erwin and H. H. Weitering, *Phys. Rev. Lett.* **81**, 2296 (1998).
- ²³R. Peierls, *Quantum Theory of Solids* (Oxford University Press, Oxford, 1955).
- ²⁴H. W. Yeom *et al.*, *Phys. Rev. Lett.* **82**, 4898 (1999).
- ²⁵J. R. Ahn, J. H. Byun, H. Koh, E. Rotenberg, S. D. Kevan, and H. W. Yeom, *Phys. Rev. Lett.* **93**, 106401 (2004).
- ²⁶S. J. Park, H. W. Yeom, S. H. Min, D. H. Park, and I.-W. Lyo, *Phys. Rev. Lett.* **93**, 106402 (2004).
- ²⁷J. R. Ahn, P. G. Kang, K. D. Ryang, and H. W. Yeom, *Phys. Rev. Lett.* **95**, 196402 (2005).
- ²⁸P. C. Snijders, S. Rogge, and H. H. Weitering, *Phys. Rev. Lett.*

- 96**, 076801 (2006).
- ²⁹J. N. Crain, M. D. Stiles, J. A. Stroschio, and D. T. Pierce, Phys. Rev. Lett. **96**, 156801 (2006).
- ³⁰J. Avila, A. Mascaraque, E. G. Michel, M. C. Asensio, G. Lelay, J. Ortega, R. Perez, and F. Flores Phys. Rev. Lett. **82**, 442 (1999).
- ³¹C. González, F. Flores, and J. Ortega, Phys. Rev. Lett. **96**, 136101 (2006).
- ³²H. W. Yeom, Phys. Rev. Lett. **97**, 189701 (2006).
- ³³C. González, F. Flores, and J. Ortega, Phys. Rev. Lett. **97**, 189702 (2006).
- ³⁴J. R. Ahn, J. H. Byun, J. K. Kim, and H. W. Yeom, Phys. Rev. B **75**, 033313 (2007).
- ³⁵D. Sánchez-Portal, P. O. E. Artacho, and J. M. Soler, Int. J. Quantum Chem. **65**, 453 (1997).
- ³⁶J. M. Soler, E. Artacho, J. D. Gale, A. García, J. Junquera, P. Ordejón, and D. Sánchez-Portal, J. Phys.: Condens. Matter **14**, 2745 (2002).
- ³⁷D. Sánchez-Portal, P. Ordejón, and E. Canadell, Struct. Bonding (Berlin) **113**, 103 (2004).
- ³⁸W. Kohn and L. Sham, Phys. Rev. **140**, 1133 (1965).
- ³⁹D. M. Ceperley and B. J. Alder, Phys. Rev. Lett. **45**, 566 (1980).
- ⁴⁰J. P. Perdew and A. Zunger, Phys. Rev. B **23**, 5048 (1981).
- ⁴¹N. Troullier and J. L. Martins, Phys. Rev. B **43**, 1993 (1991).
- ⁴²O. F. Sankey and D. J. Niklewski, Phys. Rev. B **40**, 3979 (1989).
- ⁴³J. Junquera, O. Paz, D. Sánchez-Portal, and E. Artacho, Phys. Rev. B **64**, 235111 (2001).
- ⁴⁴S. Riikonen and D. Sánchez-Portal, Phys. Rev. B **71**, 235423 (2005).
- ⁴⁵S. Riikonen and D. Sánchez-Portal, Nanotechnology **16**, 218 (2005).
- ⁴⁶S. Riikonen and D. Sánchez-Portal, Surf. Sci. **600**, 1201 (2006).
- ⁴⁷S. Riikonen, A. Ayuela, and D. Sánchez-Portal, Surf. Sci. **600**, 3821 (2006).
- ⁴⁸J. M. Haile, *Molecular Dynamics Simulation* (Wiley-Interscience, New York, 1997).
- ⁴⁹J. Tersoff and D. R. Hamann, Phys. Rev. B **31**, 805 (1985).
- ⁵⁰J. M. Perez-Mato, I. Etxebarria, S. Radescu, and S. Ivantchev, Eur. Phys. J. B **12**, 331 (1999).
- ⁵¹A. N. Rubtsov, J. Hlinka, and T. Janssen, Phys. Rev. E **61**, 126 (2000).
- ⁵²T. Aruga, Surf. Sci. Rep. **61**, 283 (2006).
- ⁵³M. Rohlfing, P. Krüger, and J. Pollmann, Phys. Rev. B **52**, 1905 (1995).
- ⁵⁴M. Rohlfing and S. G. Louie, Phys. Status Solidi A **175**, 17 (1999).
- ⁵⁵R. M. Martin, *Electronic Structure: Basic Theory and Practical Methods* (Cambridge University Press, Cambridge, 2004).
- ⁵⁶A. V. Melechko, J. Braun, H. H. Weitering, and E. W. Plummer, Phys. Rev. Lett. **83**, 999 (1999).